

17 Uniformly-fractured aquifers, double-porosity concept

17.1 Introduction

Fractures in a rock formation strongly influence the fluid flow in that formation. Conventional well-flow equations, developed primarily for homogeneous aquifers, therefore do not adequately describe the flow in fractured rocks. An exception occurs in hard rocks of very low permeability if the fractures are numerous enough and are evenly distributed throughout the rock; then the fluid flow will only occur through the fractures and will be similar to that in an unconsolidated homogeneous aquifer.

A complicating factor in analyzing pumping tests in fractured rock is the fracture pattern, which is seldom known precisely. The analysis is therefore a matter of identifying an unknown system (Section 2.9). System identification relies on models, whose characteristics are assumed to represent the characteristics of the actual system. We must therefore search for a well-defined theoretical model to simulate the behaviour of the actual system and to produce, as closely as possible, its observed response.

In recent years, many theoretical models have been developed, all of them assuming simplified regular fracture systems that break the rock mass into blocks of equal dimensions (Figure 17.1). These models usually allow conventional type-curve matching procedures to be used. But, because the mechanism of fluid flow in fractured rocks is complex, the models are complex too, comprising, as they do, several parameters or a combination of parameters. Consequently, few of the associated well functions have been tabulated, so, for the other models, one first has to calculate a set of function values. This makes such models less attractive for our purpose.

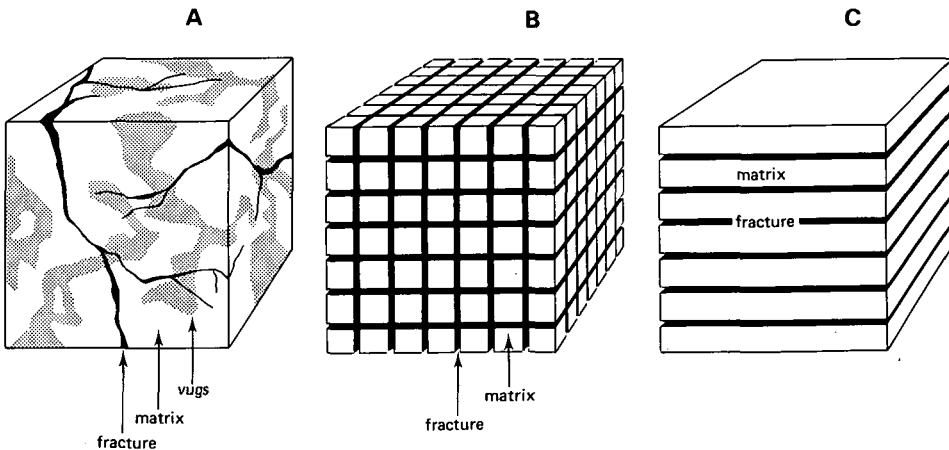


Figure 17.1 Fractured rock formations

- A: A naturally fractured rock formation
- B: Warren-Root's idealized three-dimensional, orthogonal fracture system
- C: Idealized horizontal fracture system

Even more serious is the on-going debate about fracture flow, which indicates that the theory of fluid flow in fractured media is less well-established than that in porous media. In reviewing the literature on the subject, Streltsova-Adams (1978) states: 'Published work on well tests in fractured reservoirs clearly indicates the lack of a unified approach, which has led to contradictory results in analyzing the drawdown behaviour'. And Gringarten (1982), in his review, states: 'A careful inspection of the published analytical solutions indicates that they are essentially identical. Apparent differences come only from the definition of the various parameters used in the derivation'. Indeed, in the literature, there is an enormous overlap of equations. In this chapter, therefore, we present some practical methods that do not require lengthy tables of function values and which, when used in combination, allow a complete analysis of the data to be made.

The methods we present are all based on the double-porosity theory developed initially by Barenblatt et al. (1960). This concept regards a fractured rock formation as consisting of two media: the fractures and the matrix blocks, both of them having their own characteristic properties. Two coexisting porosities and hydraulic conductivities are thus recognized: those of primary porosity and low permeability in the matrix blocks, and those of low storage capacity and high permeability in the fractures. This concept makes it possible to explain the flow mechanism as a re-equalization of the pressure differential in the fractures and blocks by the flow of fluid from the blocks into the fractures. No variation in head within the matrix blocks is assumed. This so-called interporosity flow is in pseudo-steady state. The flow through the fractures to the well is radial and in an unsteady state.

The assumption of pseudo-steady-state interporosity flow does not have a firm theoretical justification. Transient block-to-fracture flow was therefore considered by Boulton and Streltsova (1977), Najurieta (1980), and Moench (1984). From Moench's work, it is apparent that the assumption of pseudo-steady-state interporosity flow is only justified if the faces of the matrix blocks are coated by some mineral deposit (as they often are). Only then will there be little variation in head within the blocks. The pseudo-steady-state solution is thus a special case of Moench's solution of transient interporosity flow.

The methods in this chapter are all based on the following general assumptions and conditions:

- The aquifer is confined and of infinite areal extent;
- The thickness of the aquifer is uniform over the area that will be influenced by the test;
- The well fully penetrates a fracture;
- The well is pumped at a constant rate;
- Prior to pumping, the piezometric surface is horizontal over the area that will be influenced by the test;
- The flow towards the well is in an unsteady state.

The first method in this chapter, in Section 17.2, is the Bourdet-Gringarten method and its approximation, which is more universally applicable than other methods; it uses drawdown data from observation wells. Next, in Section 17.3, we present the Kazemi et al. method; it is an extension of the method originally developed by Warren

and Root (1963) for a pumped well; the Kazemi et al. method uses data from observation wells. Finally, in Section 17.4, we present the original Warren and Root method for a pumped well.

17.2 Bourdet-Gringarten's curve-fitting method (observation wells)

Bourdet and Gringarten (1980) state that, in a fractured aquifer of the double-porosity type (Figure 17.1B), the drawdown response to pumping as observed in observation wells can be expressed as

$$s = \frac{Q}{4\pi T_f} F(u^*, \lambda, \omega) \quad (17.1)$$

where

$$u^* = \frac{T_f t}{(S_f + \beta S_m) r^2} \quad (17.2)$$

$$\lambda = \alpha r^2 \frac{K_m}{K_f} \quad (17.3)$$

$$\omega = \frac{S_f}{S_f + \beta S_m} \quad (17.4)$$

f = of the fractures

m = of the matrix blocks

T = $\sqrt{T_{f(x)} T_{f(y)}}$ = effective transmissivity (m²/d)

S = storativity (dimensionless)

K = hydraulic conductivity (m/d)

λ = interporosity flow coefficient (dimensionless)

α = shape factor, parameter characteristic of the geometry of the fractures and aquifer matrix of a fractured aquifer of the double-porosity type (dimension: reciprocal area)

β = factor; for early-time analysis it equals zero and for late-time analysis it equals 1/3 (orthogonal system) or 1 (strata type)

x,y = relative to the principal axes of permeability

To avoid confusion, note that our definition of the parameter λ differs from the definition of λ commonly used in the petroleum literature; $\lambda = (r/r_w)^2 \lambda_{oil}$.

Note also that for a fracture system as shown in Figure 17.1B, $\alpha = 4n(n+2)/l^2$, where n is the number of a normal set of fractures (1, 2, or 3) and l is a characteristic dimension of a matrix block. For a system of horizontal slab blocks ($n = 1$) as shown in Figure 17.1C, $\alpha = 12/h_m^2$, where h_m is the thickness of a matrix block. Typical values of λ and ω fall within the ranges of 10^{-3} (r_w/r)² to 10^{-9} (r_w/r)² for λ and 10^{-1} to 10^{-4} for ω (Serra et al. 1983).

For small values of pumping time, Equation 17.1 reduces to

$$s = \frac{Q}{4\pi T_f} W(u) \quad (17.5)$$

where

$$u = \frac{(S_f + \beta S_m)r^2}{4 T_f t} \quad (17.6)$$

Equation 17.5 is identical to the Theis equation. It describes only the drawdown behaviour in the fracture system (β equals zero). For large values of pumping time, Equation 17.1 also reduces to the Theis equation, which now describes the drawdown behaviour in the combined fracture and block system (β equals 1/3 or 1).

According to the pseudo-steady-state interporosity flow concept, the drawdown becomes constant at intermediate pumping times when there is a transition from fracture flow to flow from fractures and matrix blocks. The drawdown at which the transition occurs is equal to

$$s = \frac{Q}{2\pi T_f} K_0(\sqrt{\lambda}) \quad (17.7)$$

where $K_0(x)$ is the modified Bessel function of the second kind and of zero order.

Bourdet and Gringarten (1980) showed that, for λ values less than 0.01, Equation 17.7 reduces to

$$s = \frac{2.30Q}{4\pi T_f} \log \frac{1.26}{\lambda} \quad (17.8)$$

The drawdown at which the transition occurs is independent of early- and late-time drawdown behaviours and is solely a function of λ .

Bourdet and Gringarten (1980) presented type curves of $F(u^*, \lambda, \omega)$ versus u^* for different values of λ and ω (Figure 17.2). These type curves are obtained as a superposition of Theis solutions labelled in ω values, with a set of curves representing the behaviour during the transitional period and depending upon λ .

As can be seen from Figure 17.2, the horizontal segment does not appear in the type curves at high values of ω . For high ω values, the type curves only have an inflection point. Numerous combinations of ω and λ values are possible, each pair yielding different type curves. But, instead of presenting extensive tables of function values required to prepare these many different type curves, we present a simplified method. It is based on matching both the early- and late-time data with the Theis type curve, which yields values of T_f and S_f , and T_f and $S_f + S_m$, respectively. From the steady-state drawdown at intermediate times, a value of λ can be estimated from Equation 17.7 or 17.8.

The Bourdet-Gringarten method can be used if, in addition to the general assumptions and conditions listed in Section 17.1, the following assumptions and conditions are satisfied:

- The aquifer is of the double-porosity type and consists of homogeneous and isotropic blocks or strata of primary porosity (the aquifer matrix), separated from each other either by an orthogonal system of continuous uniform fractures or by equally-spaced horizontal fractures;
- Any infinitesimal volume of the aquifer contains sufficient portions of both the aquifer matrix and the fracture system;

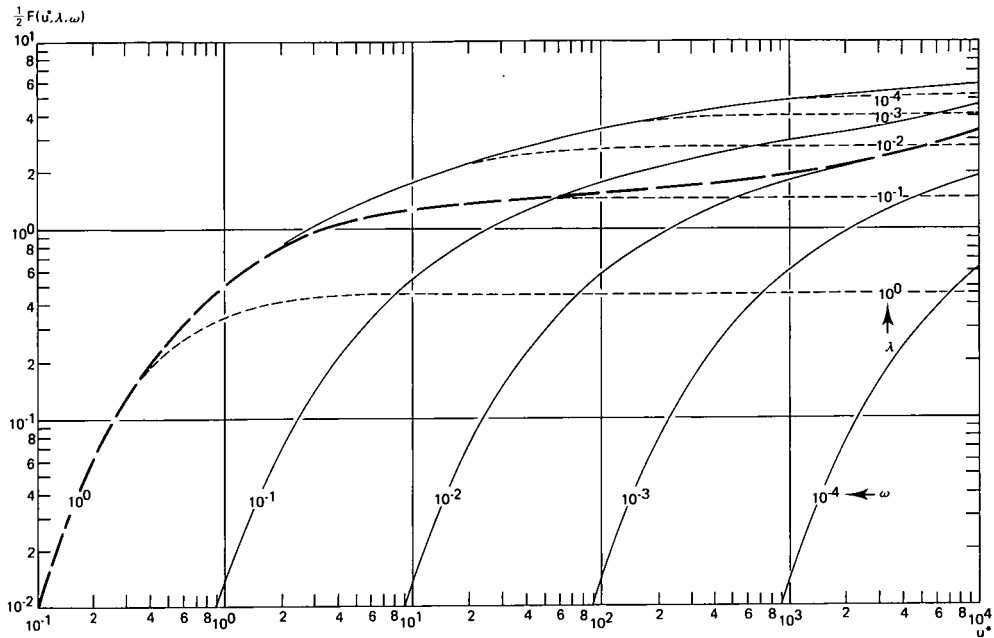


Figure 17.2 Type curves for the function $F(u^*, \lambda, \omega)$ (after Bourdet and Gringarten 1980)

- The aquifer matrix has a lower permeability and a higher storativity than the fracture system;
- The flow from the aquifer matrix into the fractures (i.e. the interporosity flow) is in a pseudo-steady state;
- The flow to the well is entirely through the fractures, and is radial and in an unsteady state;
- The matrix blocks and the fractures are compressible;
- $\lambda < 1.78$.

Bourdet and Gringarten (1980) showed that the double-porosity behaviour of a fractured aquifer only occurs in a restricted area around the pumped well. Outside that area (i.e. for λ values greater than 1.78), the drawdown behaviour is that of an equivalent unconsolidated, homogeneous, isotropic confined aquifer, representing both the fracture and the block flow.

Procedure 17.1

- Prepare a type curve of the Theis well function on log-log paper by plotting values of $W(u)$ versus $1/u$, using Annex 3.1;
- On another sheet of log-log paper of the same scale, plot the drawdown s observed in an observation well versus the corresponding time t ;
- Superimpose the data plot on the type curve and adjust until a position is found where most of the plotted points representing the early-time drawdowns fall on the type curve;

- Choose a match point A and note the values of the coordinates of this match point, $W(u)$, $1/u$, s , and t ;
- Substitute the values of $W(u)$, s , and Q into Equation 17.5 and calculate T_f ;
- Substitute the values of $1/u$, T_f , t , and r into Equation 17.6 and calculate S_f ($\beta = 0$);
- If the data plot exhibits a horizontal straight-line segment or only an inflection point, note the value of the stabilized drawdown or that of the drawdown at the inflection point. Substitute this value into Equation 17.7 or 17.8 and calculate λ ;
- Now superimpose the late-time drawdown data plot on the type curve and adjust until a position is found where most of the plotted points fall on the type curve;
- Choose a matchpoint B and note the values of the coordinates of this matchpoint, $W(u)$, $1/u$, s , and t ;
- Substitute the values of $W(u)$, s , and Q into Equation 17.5 and calculate T_f ;
- Substitute the values of $1/u$, T_f , t , and r into Equation 17.6 and calculate $S_f + S_m$ ($\beta = 1/3$ or 1).

Remarks

- For relatively small values of ω , matching the late-time drawdowns with the Theis type curve may not be possible and the analysis will only yield values of T_f and S_f ;
- For high values of λ (i.e. for large values of r), the drawdown in an observation well no longer reflects the aquifer's double-porosity character and the analysis will only yield values of T_f and $S_f + S_m$;
- Gringarten (1982) pointed out that the Bourdet-Gringarten's type curves are identical to the time-drawdown curves for an unconsolidated unconfined aquifer with delayed yield as presented by Boulton (1963). (See also Chapter 5.) If one has no detailed knowledge of the aquifer's hydrogeology, this may lead to a misinterpretation of the pumping test data.

17.3 Kazemi et al.'s straight-line method (observation wells)

Kazemi et al. (1969) showed that the drawdown equations developed by Warren and Root (1963) for a pumped well can also be used for observation wells. Their extension of the approximation of the Warren-Root solution is, in fact, also an approximation of the general solution of Bourdet and Gringarten (1980). It can be expressed by

$$s = \frac{Q}{4\pi T_f} F(u^*, \lambda, \omega) \quad (17.1)$$

where

$$F(u^*, \lambda, \omega) = 2.3 \log(2.25 u^*) + \text{Ei}\left(-\frac{\lambda u^*}{\omega(1-\omega)}\right) - \text{Ei}\left(-\frac{\lambda u^*}{1-\omega}\right) \quad (17.9)$$

Equation 17.9 is valid for u^* values greater than 100, in analogy with Jacob's approximation of the Theis solution (Chapter 3).

A semi-log plot of the function $F(u^*, \lambda, \omega)$ versus u^* (for fixed values of λ and ω) will reveal two parallel straight lines connected by a transitional curve (Figure 17.3). Consequently, the corresponding s versus t plot will theoretically show the same pattern (Figure 17.4).

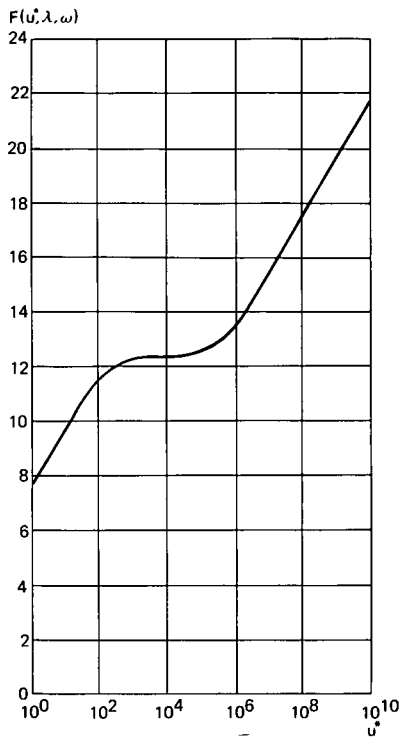


Figure 17.3 Semi-log plot of the function $F(u^*, \lambda, \omega)$ versus u^* for fixed values of λ and ω

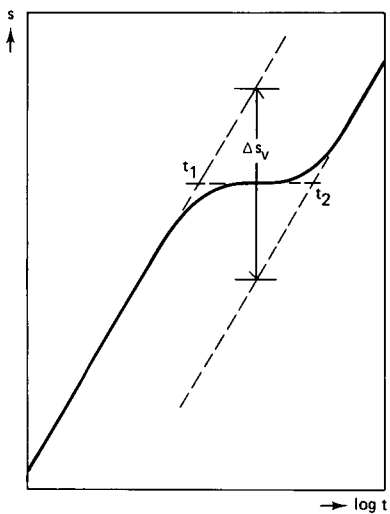


Figure 17.4 Semi-log time-drawdown plot for an observation well in a fractured rock formation of the double-porosity type

For *early pumping times*, Equations 17.1 and 17.9 reduce to

$$s = \frac{2.30Q}{4\pi T_f} \log \frac{2.25 T_f t}{S_f r^2} \quad (17.10)$$

Equation 17.9 is identical to Jacob's straight-line equation (Equation 3.7). The water flowing to the well during early pumping times is derived solely from the fracture system ($\beta = 0$).

For *late pumping times*, Equations 17.1 and 17.9 reduce to

$$s = \frac{2.30Q}{4\pi T_f} \log \frac{2.25 T_f t}{(S_f + \beta S_m) r^2} \quad (17.11)$$

Equation 17.11 is also identical to Jacob's equation. The drawdown response, however, is now equivalent to the response of an unconsolidated homogeneous isotropic aquifer whose transmissivity equals the transmissivity of the fracture system, and whose storativity equals the arithmetic sum of the storativity of the fracture system and that of the aquifer matrix. Hence, the water flowing to the well at late pumping times comes from both the fracture system and the aquifer matrix.

Kazemi et al.'s method is based on the occurrence of the two parallel straight lines in the semi-log data plot. Whether these lines appear in such a plot depends solely on the values of λ and ω . According to Mavor and Cinco Ley (1979), Equation 17.10, describing the early-time straight line, can be used if

$$u^* \leq \frac{\omega(1-\omega)}{3.6 \lambda} \quad (17.12)$$

and Equation 17.11, describing the late-time straight line, can be used if

$$u^* \geq \frac{1-\omega}{1.3 \lambda} \geq 100 \quad (17.13)$$

If the two parallel straight lines occur in a semi-log data plot, the value of ω can be derived from the vertical displacement of the two lines, Δs_v , and the slope of these lines, Δs (Figure 17.4).

$$\omega = 10^{-\Delta s_v / \Delta s} \quad (17.14)$$

According to Mavor and Cinco Ley (1979), the value of ω can also be estimated from the horizontal displacement of the two parallel straight lines (Figure 17.4)

$$\omega = t_1 / t_2 \quad (17.15)$$

Following the procedure of the Jacob method on both straight lines in Figure 17.4, we can determine values of T_f , S_f , and S_m . Using Equation 17.7 or 17.8, we can estimate the value of λ from the constant drawdown at intermediate times.

Kazemi et al.'s method can be used if, in addition to the assumptions and conditions underlying the Bourdet-Gringarten method, the condition that the value of u^* is larger than 100 is satisfied.

According to Van Golf-Racht (1982), the condition $u^* > 100$ is very restrictive and can be replaced by $u^* > 100 \omega$, if $\lambda \ll 1$, or by $u^* > 100 - 1/\lambda$, if $\omega \ll 1$.

Procedure 17.2

- On a sheet of semi-log paper, plot s versus t (t on logarithmic scale);
- Draw a straight line through the early-time points and another through the late-time points; the two lines should plot as parallel lines;
- Determine the slope of the lines (i.e. the drawdown difference Δs per log cycle of time);
- Substitute the values of Δs and Q into $T_r = 2.30 Q/4\pi \Delta s$, and calculate T_r ;
- Extend the early-time straight line until it intercepts the time axis where $s = 0$, and determine t_1 ;
- Substitute the values of T_r , t_1 , and r into $S_r = 2.25 T_r t_1/r^2$, and calculate S_r ;
- Extend the late-time straight line until it intercepts the time axis where $s = 0$, and determine t_2 ;
- Substitute the values of T_r , t_2 , r , and β into $S_r + \beta S_m = 2.25 T_r t_2/r^2$, and calculate $S_r + S_m$;
- Calculate the separate values of S_r and S_m .

Remarks

The two parallel straight lines can only be obtained at low λ values (i.e. $\lambda < 10^{-2}$). At higher λ values, only the late-time straight line, representing the fracture and block flow, will appear, provided of course that the pumping time is long enough. The analysis then yields values of T_r and $S_r + S_m$.

To obtain separate values of S_r and S_m when only one straight line is present, Procedure 17.3 can be applied.

Procedure 17.3

- Follow Procedure 17.2 to obtain values of T_r and S_r from the first straight line, or if it is not present, values of T_r and $S_r + S_m$ from the second straight line;
- Determine the centre of the transition period of constant drawdown and determine $1/2 \Delta s_v$;
- Calculate the value of ω using Equation 17.14;
- Substituting the values of ω and β into Equation 17.4, determine the value of S_m if S_r is known, or vice versa.

Remark

To estimate the centre of the transition period with constant drawdown, the preceding and following curved-line segments should be present in the time-drawdown plot.

17.4 Warren-Root's straight-line method (pumped well)

As Kazemi et al.'s straight-line method for observation wells is an extension of Warren-Root's straight-line method for a pumped well, we can use Equations 17.7 to 17.15 to analyze the drawdown in a pumped well if we replace the distance of the observation well to the pumped well, r , with the effective radius of the pumped well, r_w .

Following Procedure 17.2 on both straight lines in the semi-log plot of s_w versus t , we can determine T_r , S_r , and S_m , provided that there are no well losses (i.e. no skin) and that well-bore storage effects are negligible.

According to Mavor and Cinco Ley (1979), well-bore storage effects become negligible when

$$u^* > C' (60 + 3.5 \text{ skin}) \quad (17.16)$$

where, at early pumping times

$$C' = C/2\pi S_r r_w^2 \text{ (dimensionless)}$$

C = well-bore storage constant = ratio of change in volume of water in the well and the corresponding drawdown (m^3)

For a water-level change in a perfect well (i.e. no well losses), which is pumping a homogeneous confined aquifer, the dimensionless coefficient C' is related to the dimensionless α as defined by Papadopoulos (1967) (see Section 11.1.1) by the relationship (Ramey 1982)

$$C' = 1/2\alpha$$

When well-bore storage effects are not negligible, the limiting condition for applying Equation 17.10, as expressed by Equation 17.12, should be replaced by

$$C' (60 + 3.5 \text{ skin}) < u^* < \frac{\omega(1-\omega)}{3.6 \lambda} \quad (17.17)$$

The early-time straight line may thus be obscured by storage effects in the well and in the fractures intersecting the well. But, with Procedure 17.3, a complete analysis is then still possible.

Remarks

Well losses (skin) do not influence the calculation of T_r and ω .

If the linear well losses are not negligible, Equation 17.8 becomes (Bourdet and Gringarten 1980)

$$s_w = \frac{2.30Q}{4\pi T_r} \log \frac{1.26}{\lambda e^{-2\text{skin}}} \quad (17.18)$$

From the constant drawdown s_w and the calculated value of T_r , the value of $\lambda e^{-2\text{skin}}$ can be determined. If the well losses are known or negligible, the value of λ can be estimated.

Example 17.1

For this example, we use the time-drawdown data from Pumping Test 3 conducted on Well UE-25b # 1 in the fractured Tertiary volcanic rocks of the Nevada Test Site, U.S.A., as published by Moench (1984).

The well ($r_w = 0.11$ m; total depth 1219 m) was drilled through thick sequences of fractured and faulted non-welded to densely welded rhyolitic ash flow and bedded tuffs to a depth below the watertable, which was struck at 470 m below the ground surface. Five major zones of water entry occurred over a depth interval of 400 m. The distance between these zones was roughly 100 m. Core samples revealed that most of the fractures dip steeply and are coated with deposits of silica, manganese, and iron oxides, and calcite. The water-producing zones, however, had mineral-filled low-angle fractures, as observed in core samples taken at 612 m below the ground surface.

The well was pumped at a constant rate of 35.8 l/s for nearly 3 days. Table 17.1 shows the time-drawdown data of the well.

Like Moench, we assume that the fractured aquifer is unconfined and of the strata type (i.e. $\beta = 1$). Figure 17.5 shows the log-log drawdown plot of the pumped well and Figure 17.6 the semi-log drawdown plot. These figures clearly reveal the double porosity of the aquifer because they show the early-time, intermediate-time, and late-time segments characteristic of double-porosity media. At early pumping times, however, well-bore storage affects the time-drawdown relationship of the well. In a log-log plot of drawdown versus time, well-bore storage is usually reflected by a straight line of slope unity. Consequently, the two parallel straight lines of the Warren and Root model do not appear in Figure 17.6. Only the late-time data plot as a straight line.

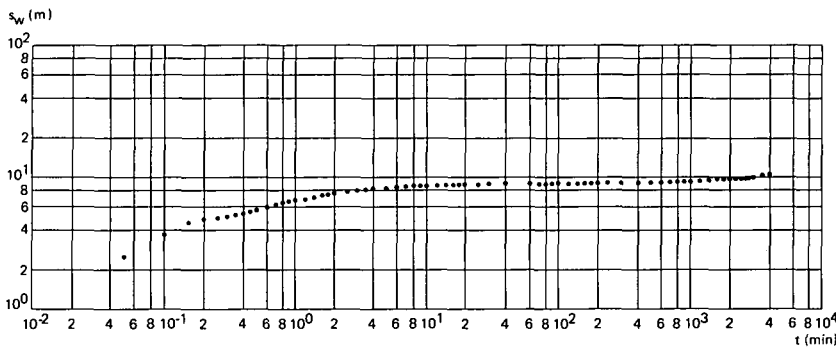


Figure 17.5 Time-drawdown log-log plot of data from the pumped well UE-25b#1 at the Nevada Test Site, U.S.A. (after Moench 1984)

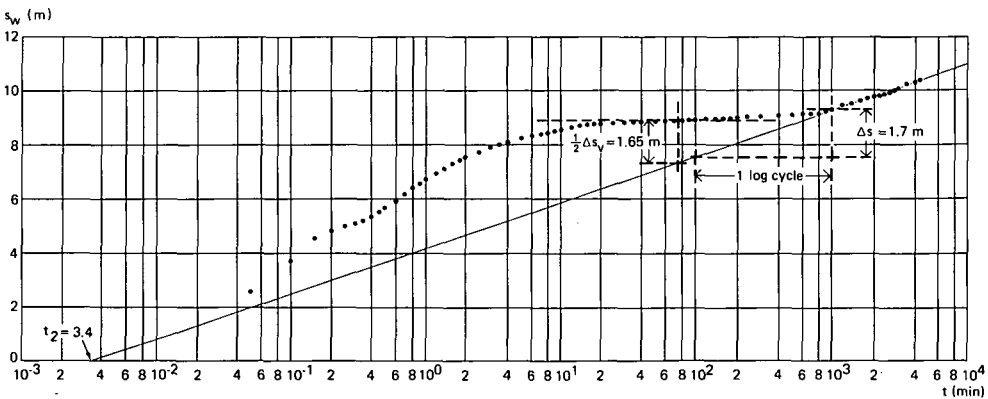


Figure 17.6 Time-drawdown semi-log plot of data from the pumped well UE-25b#1 at the Nevada Test Site, U.S.A. (after Moench 1984)

Well-bore skin effects are unlikely, because air was used when the well was being drilled, the major water-producing zones were not screened, and prior to testing the well was thoroughly developed.

To analyze the drawdown in this well, we follow Procedure 17.3. From Figure 17.6, we determine the slope of the late-time straight line, which is $\Delta s = 1.70$ m. We then calculate the fracture transmissivity from

$$T_f = \frac{2.30Q}{4\pi\Delta s} = \frac{2.3 \times 3093.12}{4 \times 3.14 \times 1.70} = 333 \text{ m}^2/\text{d}$$

Table 17.1 Drawdown data from pumped well UE-25b #1, test 3 (after Moench 1984)

t (min)	s _w (m)	t (min)	s _w (m)
0.05	2.513	30.0	8.84
0.1	3.769	35.0	8.84
0.15	4.583	40.0	8.86
0.2	4.858	50.0	8.86
0.25	5.003	60.0	8.90
0.3	5.119	70.0	8.91
0.35	5.230	80.0	8.92
0.4	5.390	90.0	8.93
0.45	5.542	100.0	8.95
0.5	5.690	120.0	8.97
0.6	5.990	140.0	8.98
0.7	6.19	160.0	8.99
0.8	6.42	180.0	9.00
0.9	6.59	200.0	9.02
1.0	6.74	240.0	9.04
1.2	6.96	300.0	9.07
1.4	7.17	400.0	9.11
1.6	7.33	500.0	9.14
1.8	7.45	600.0	9.17
2.0	7.56	700.0	9.18
2.5	7.76	800.0	9.21
3.0	7.93	900.0	9.25
3.5	8.03	1000.0	9.30
4.0	8.12	1200.0	9.44
5.0	8.24	1400.0	9.55
6.0	8.32	1600.0	9.64
7.0	8.41	1800.0	9.74
8.0	8.46	2000.0	9.78
9.0	8.54	2200.0	9.80
10.0	8.62	2400.0	9.84
12.0	8.67	2600.0	9.93
14.0	8.70	2800.0	10.03
16.0	8.74	3000.0	10.08
18.0	8.76	3500.0	10.26
20.0	8.77	4000.0	10.30
25.0	8.81	4200.0	10.41

Extending the straight line until it intercepts the time axis where $s = 0$ yields $t_2 = 3.4 \times 10^{-3}$ min. The overall storativity is then calculated from

$$S_f + S_m = \frac{2.25 T_f t_2}{r_w^2} = \frac{2.25 \times 333 \times 3.4 \times 10^{-3}}{1440 (0.11)^2} = 0.15$$

The semi-log plot of time versus drawdown shows that the centre of the transition period is at $t \approx 75$ minutes. At $t = 75$ minutes, $1/2 \Delta s_v = 1.65$ m. Substituting the appropriate values into Equation 17.14 yields

$$\omega = 10^{-\Delta s_v / \Delta s} = 10^{-2 \times 1.65 / 1.70} = 0.011$$

Substituting the appropriate values into Equation 17.4 yields

$$S_f = \omega (S_f + S_m) = 0.011 \times 0.146 = 0.0016$$

and

$$S_m = 0.15$$

This high value of S_m is an order of magnitude normally associated with the specific yield of unconfined aquifers. Moench (1984), however, offers an explanation for such a high value for the storativity of the fractured volcanic rock, namely that it may be due to the presence of highly compressible microfissures within the matrix blocks. We consider this a plausible explanation, because there is little reason to assume homogeneous matrix blocks, as in Figure 17.1C.

We must now check the condition that $u^* > 100$, which underlies the Warren-Root method. Substituting the appropriate values into Equation 17.2, we obtain

$$t > \frac{100 (S_f + S_m) r_w^2}{T_f} = \frac{100 \times 1440 \times 0.15 (0.11)^2}{333} = 0.8 \text{ min}$$

Hence this condition is satisfied.

Next, we must check the condition stated in Equation 17.13. For this, we need the value of λ . The constant drawdown during intermediate times is taken as 8.9 m. Using Equation 17.8, we obtain

$$\lambda = 1.26 / 10^{(4 \times 3.14 \times 333 \times 8.9) / (2.3 \times 3093.12)} = 7.3 \times 10^{-6}$$

Substituting the appropriate values into Equation 17.13 gives

$$t > \frac{(1-\omega) S_f + S_m}{1.3 \lambda T_f} r_w^2 = \frac{1440 (1-0.011) 0.15 (0.11)^2}{1.3 \times 7.3 \times 10^{-6} \times 333} = 818 \text{ min}$$

The condition for the second straight-line relationship is also satisfied.

Finally, we must check our assumption that the first straight-line relationship is obscured by well-bore storage effects. Using $C' = 1/2\alpha$ and assuming $r_c = r_w$ gives us $C' = 1/2S_f$. Taking this C' value and using Equation 17.16, we get

$$t > \frac{60 r_w^2}{2 T_f} = \frac{1440 \times 60 (0.11)^2}{2 \times 333} = 1.6 \text{ min}$$

So, according to Equation 17.16, after approximately 1.6 min, the drawdown data are no longer influenced by well-bore storage effects. A check of Figure 17.6 shows us that the early-time straight-line relationship would have occurred before then and is thus obscured by well-bore storage effects.

